



ISSN: 0067-2904

Synthesis and Characterisation of Zinc-doped Antimony Selenide

Thamir A. Jumah¹, Riyadh K. Chillab², Kassim M. Wadi¹, Hikmat N. Abdul-Kareem¹

¹Al-Nahrain University, College of Sciences, Baghdad, Iraq

²Al-Mamoon University College, Baghdad, Iraq

Received: 16/8/2020

Accepted: 16/5/2021

Abstract

Antimony selenide substituted with $Sb_{0.4}Se_{0.6}$ and doped with zinc at three doping ratios ($x=0, 0.01$ and 0.03) was prepared via the solid state reaction method. The three prepared compositions were reacted thermally at $400\text{ }^{\circ}\text{C}$ for 3 h. The structure of specimens was characterised via X-ray powder diffractometer to obtain the type of crystalline structure and lattice parameters of the prepared specimens, which showed a polycrystalline, orthorhombic structure. Optical characterisation was then achieved via UV-visible spectroscopy to exhibit the transmittance and reflectance spectra and estimate the band gap values of the prepared compositions. The samples showed high absorption spectra at low wavelengths (from 60% to 90%) and low reflectance values (from nearly zero to 17%). The band gap measurement showed an indirect transition, with values ranging from 1.2 eV to 1.23 eV. The electrical characteristics were represented by DC resistivity measurement at low temperature and AC conductivity measurement against frequency. The compositions showed a semiconducting behaviour in DC resistivity and compatible results in AC conductivity.

Keywords: Antimony selenide, Solid state reaction, Absorbance spectrum, AC conductivity, DC resistivity, Band gap, Indirect transition.

تصنيع و توصيف مركب سيلينيوم-انتيمون المشوب بالزنك

ثامر عبد الجبار جمعة¹، رياض كامل جلاب، قاسم مهدي وادي، حكمت نجيب عبد الكريم،

¹قسم الفيزياء، كلية العلوم، جامعة النهرين، بغداد، العراق

²كلية المأمون الجامعة، قسم هندسة السيطرة، بغداد، العراق

الخلاصة

تم تشويب مركب سيلينيوم-انتيمون بوساطة الزنك وبالنسب التالية (0%، 0.01%، 0.03%) وبثلاث مجاميع وحضرت جميعها بطريقة تفاعل الحالة الصلبة عند درجة حرارة 400 درجة مئوية و لمدة ثلاث ساعات. تم توصيف المركبات الناتجة بوساطة تقنية الاشعة السينية المحادة فوجدت ذات تركيب بلوري Orthorhombic وكذلك ايجاد ثوابت الخلية للنماذج المحضرة. تم توصيف النماذج المحضرة بصريا بوساطة تقنية الاشعة فوق البنفسجية - المرئية لبيان طيف الامتصاصية و الانعكاسية و استنباط فجوة الطاقة . تبين قدرة تلك النماذج على امتصاص عالية للأطوال الموجية الواطئة ونسبة تراوحت بين 60%---90% بينما تراوح طيف الانعكاس من 0%---17% و بينت النتائج حصول حالة الانتقال غير المباشر وان قيمة فجوة الطاقة تراوحت بين 1.2 إلكترون فولت--- 1.23 إلكترون فولت. تم تشخيص الخواص الكهربائية من

خلال فحص مقاومة دائرة التيار المستمر عند درجات حرارة منخفضة كذلك دراسة توصيلية دائرة التيار المتناوب كدالة للتردد فوجدت بان جميع النماذج تتصرف كأشباه موصلات في كلا الدائرتين.

1- Introduction

Semiconductor selenides are widely used in various industrial applications, such as solar cells, sensors, optical filters, and laser materials [1]. An antimony selenide (Sb_2Se_3) semiconductor is a considerable member of the V_2VI_3 compound group which has an orthorhombic crystalline structure and layer-structured form. This type of semiconductor material has high thermoelectric power and efficient photovoltaic characteristics, and can potentially be applied into thermoelectric and optical cooling devices [2,3]. Studies on the effects of doping agents or impurities on the physical properties of Sb_2Se_3 materials are considerably important in basic and practical researches [4-8]. The aim of this study is the synthesis of semiconductor selenides, by doping the enhanced metal through solid state reaction, and studying their structural, optical, and electrical characteristics. For this purpose, Sb_2Se_3 with $\text{Sb}_{0.4}\text{Se}_{0.6}$ was doped in different ratios with Zn^{2+} via solid state reaction.

2- Materials and methods

Each of Sb (121.760g/mol) and Se (78.96g/mol) with molar ratios of 0.4 mol% and 0.6 mol%, respectively, were mixed carefully with Zn^{2+} in doping ratios of $x=0$, 0.01wt.% and 0.03 wt%. Initially, these amounts were placed in an agate mortar for mixing. The second step was adding 5 ml of ethanol alcohol, followed by careful mixing for 1 h to homogenise the precursors. The mixture was dried in an oven at a temperature of 80 °C for 1 h. Solid state reaction was achieved by transporting the mixed wet powders into a silica crucible and fired at 400 °C for 3 h to achieve calcination. The calcined powder was crushed in the mortar and compacted into pellets with a diameter of 1 cm by applying a pressure of 250 MPa. These pellets were annealed at 200 °C. The geometrical densities of these prepared pellets were measured after being fired for 1 hour. Finally, the annealed specimens were prepared for electrical measurement represented by DC and AC conductivity via four-point probe technique. This type of measurement was achieved using a Wayne Kerr 6500 LCR meter with a specialised cell under various frequencies, ranging from 10 Hz to 120 MHz, at a constant temperature of 300 K. The optical measurement was represented by UV-visible spectroscopy. The wavelength ranged from 200 nm to 800 nm as in the spectroscopy setting.

3- Results and Discussion

3.1- X-ray diffraction analysis

Due to solid state reaction type (solid + solid =solid) between the reactanting components, this reaction may be produce new compositions. Thus, the x-ray diffraction test was achieved, as shown in Figure 1. The x-ray pattern provided qualitative and quantitative analyses via comparison with the XRD of the original composition file (98-001-6680) from the Inorganic Crystal Structure Database. Slight in-peak positions, which represent the presence of Zn^{2+} impurities in the doped samples, were revealed. Accordingly, the XRD pattern showed an orthorhombic structure with a space group (p n m a). XRD results showed that no other phase was formed with the Sb_2Se_3 phase, which proved the stoichiometry of the reacted precursors and, hence, no chemical bonds were formed [8].

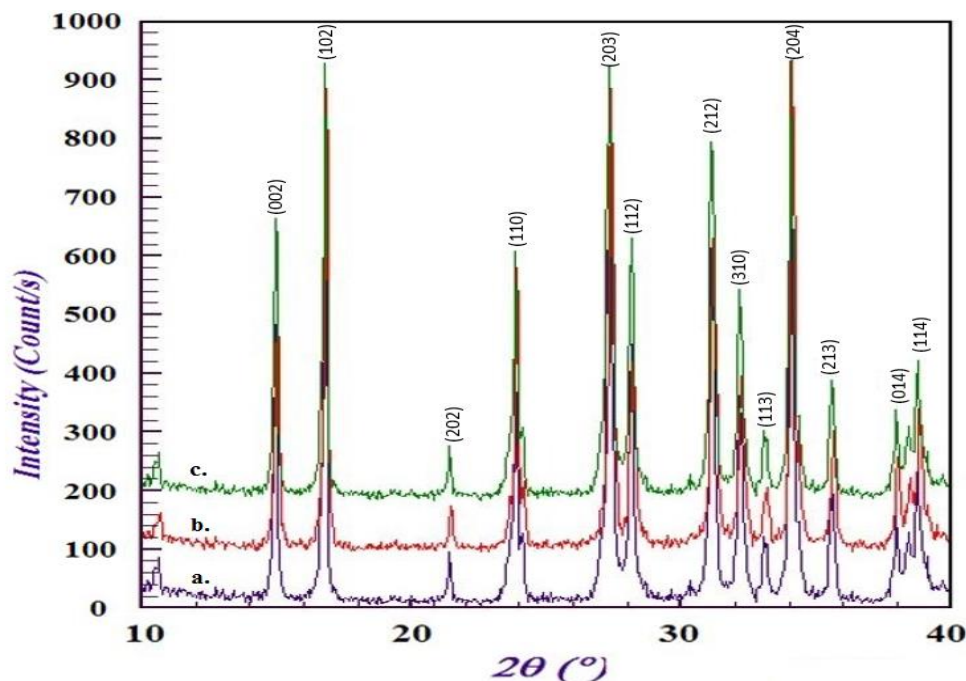


Figure 1- XRD pattern of $Sb_{0.4}Se_{0.6}Zn_x$ samples. Curve **a**: $x=0$, curve **b**: $x=0.01$ and curve **c**: $x=0.03$.

Lattice parameter values were evaluated using the Rietveld refinement FullProf software and are listed in Table 1. Lattice constant values decreased with the increase in Zn^{2+} content. The values of unit cell volume were found to be lower than that in the software’s standard pattern. The difference in values may refer to the inhomogeneous preparation in comparison to the standard operation conditions.

Table 1- Unit cell parameters of $Sb_{0.4}Se_{0.6}Zn_x$ samples

Parameter	$x=0$	$x=0.01$	$x=0.03$
a (Å)	11.604	11.648	11.587
b (Å)	3.946	3.968	3.951
c (Å)	11.759	11.768	11.749
V (Å ³)	538.4	543.9	537.9

3.2 Optical characteristics

When various prepared specimens were subjected to optical analyses by previous researches, it was found that the band gap of Sb_2Se_3 has opposite behaviours related to direct and indirect transitions. Several values of band gap were listed in these reports, with varied ranges of effective energy values. For instance, Rodrigues-Lazcano reported thin films with an indirect band gap of 1–1.2 eV, which can be derived from the equation (1) stated below [9].

$$\alpha h\nu = [h\nu - E_g]^r \dots\dots\dots(1)$$

where (α) is the absorption coefficient and r refers to the direct and indirect transition.

Rajpure *et al.* presented Sb_2Se_3 polycrystalline films with a direct band gap of 2.14 eV. [10]. El-Sayed *et al.* stated indirect and direct energy gaps in magnitudes of 1.15 and 1.5 eV, respectively [11,12]. Information on the optical characteristics of the samples under study was

obtained by measuring the absorbance and transmittance spectra, as shown in Figure 2a,b,c [12].

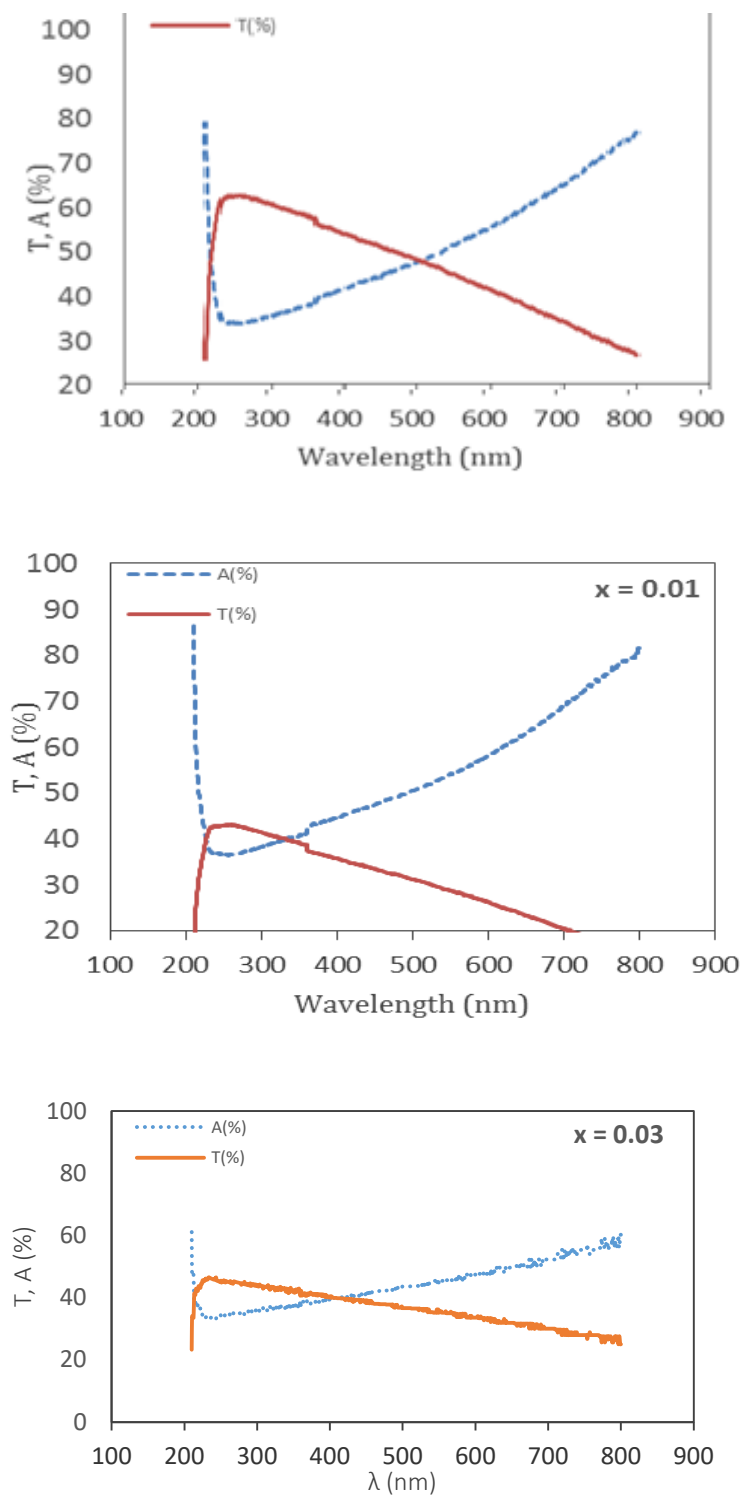


Figure 2-Transmittance and absorbance spectra of $Sb_{0.4}Se_{0.6}Zn_x$ samples for a) $x=0$, b) $x=0.01$, and c) $x=0.03$.

The absorbance values in wavelengths <400 nm were high (nearly 90% in $x=0.01$ composition), whereas transmittance had low values. In Figure 2, the behaviours of the absorbance and transmittance spectra seemed to be the same for all the compositions, but with

different values. The results showed high absorbance at low wavelengths. This variation is related to the doping effect of zinc with antimony and selenium. The value of reflectance can be evaluated according to the following equation:

$$R = 1 - T - A, \dots\dots\dots (2)$$

These compositions exhibited low reflectance, which ranged between nearly zero to a maximum value of $x=0.03$, that is, 17%. The optical transmission measurements showed an indirect transition for all the samples (Figures 3-a, b and c).

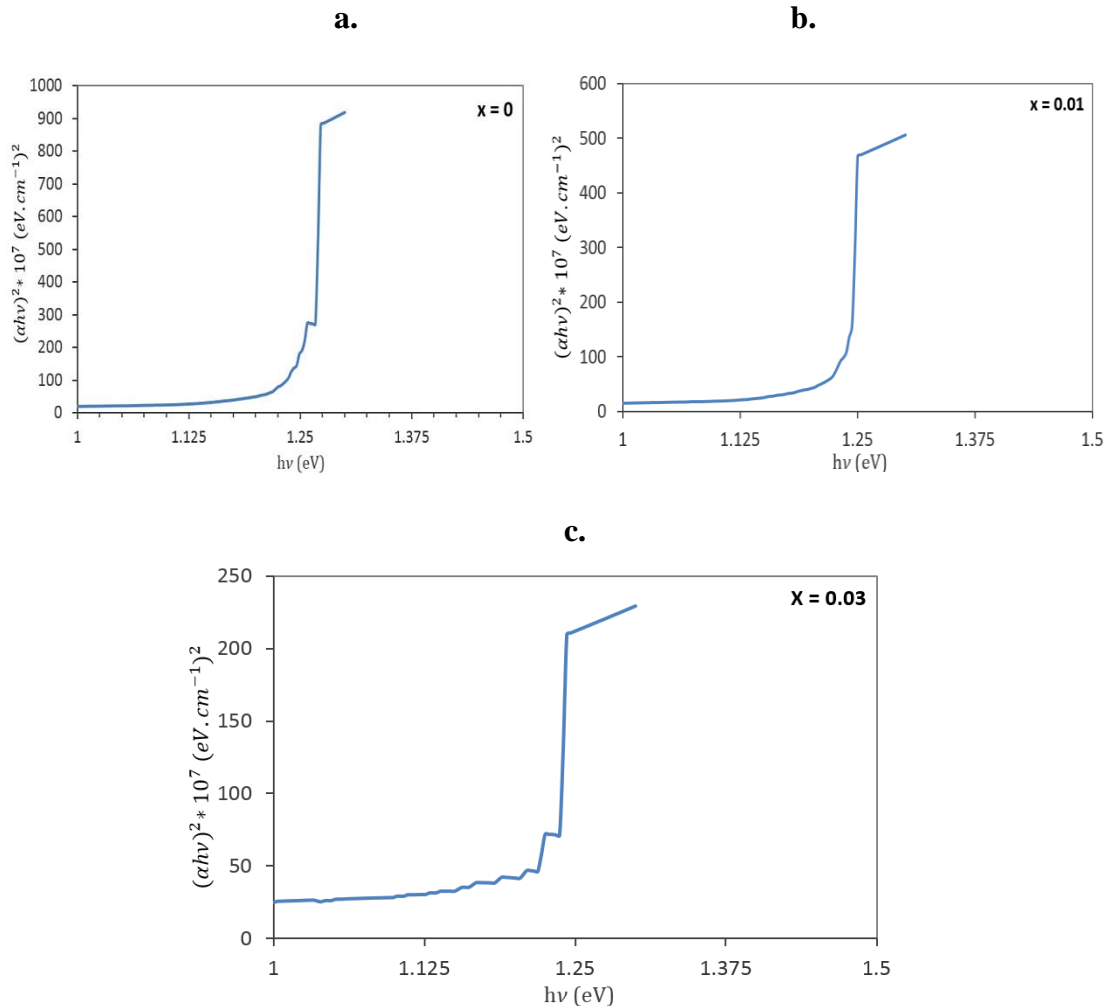


Figure 3-Plots of $(\alpha h\nu)^2$ against $h\nu$ for $Sb_{0.4}Se_{0.6}Zn_x$ samples at a) $x=0$, b) $x=0.01$, and c) $x=0.03$.

The band gap (E_g) values decreased from 1.23 eV for $x=0$ and 1.22 eV for $x=0.01$ to 1.2 eV for $x=0.03$, as stated in Table 2. Therefore, energy gap values decrease with the increase in doping ratio.

Table 2-Energy gap against doped concentration

Zinc concentration	Energy gap
X=0	1.23 eV
X=0.01	1.22 eV
X=0.03	1.2 eV

3.3 Electrical measurements

The DC resistivity was plotted against temperature, as shown in Figure 4. The low temperature-dependent DC resistivity (ρ_{DC}) measurement was achieved using a four-point-

probe cryogenic system. The temperature ranged from 5 to 300 K. The resistivity behaviour showed a basic characteristic as a semiconductor, in which the values of ρ increased with the decrease in temperature for the prepared samples. These results referred to the principle behaviour of semiconductor where the resistivity is enhanced when the temperature is increased. Moreover, the values of DC resistivity increased with the presence of the doping element (zinc). The D.C. conductivity ($\sigma_{d.c.}$) was calculated according to the following equation:

$$\sigma_{d.c.} = L / R.A = 1 / \rho \dots\dots\dots(3)$$

where σ is conductivity, ρ is resistivity, L is distance between electrodes, R is resistance, and A is cross section area. Whereas the A.C. conductivity ($\sigma_{a.c.}$) was calculated according to the following equation:

$$B(\omega) = G(\omega) d / A \dots\dots\dots (4)$$

where $G(\omega)$ is conductance, d is thickness, and A is cross section area of the electrode.

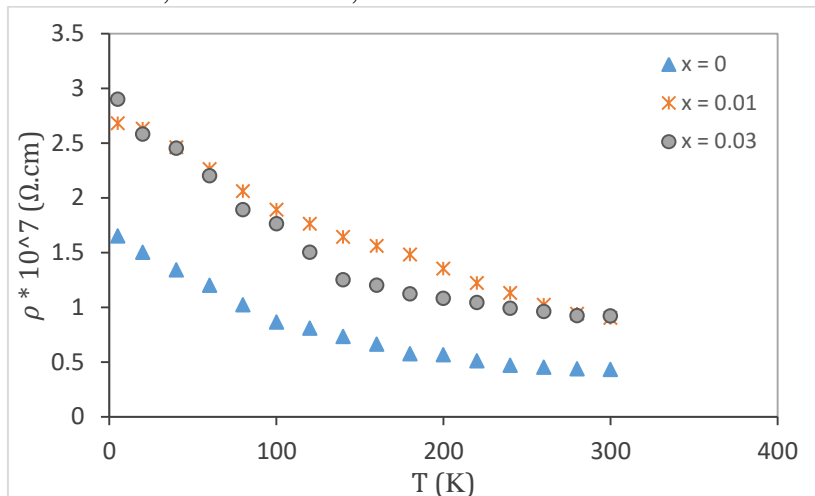


Figure 4. DC resistivity (ρ_{DC}) measurement with temperature for $Sb_{0.4}Se_{0.6}Zn_x$ samples

The AC conductivity (σ_{AC}) measurements are presented in Figure 5. Frequency values were graphed in a logarithmic form of angular frequency (ω) to eliminate zeros from the frequency scale. The samples under study showed a reduction in the values of AC conductivity when the frequency increased. However, at high frequencies (30–40 MHz.), an increase in σ_{AC} values was observed, which may indicate an electronic or vibrational response [13,14]. Ren *et al.* reported similar results in some details [15].

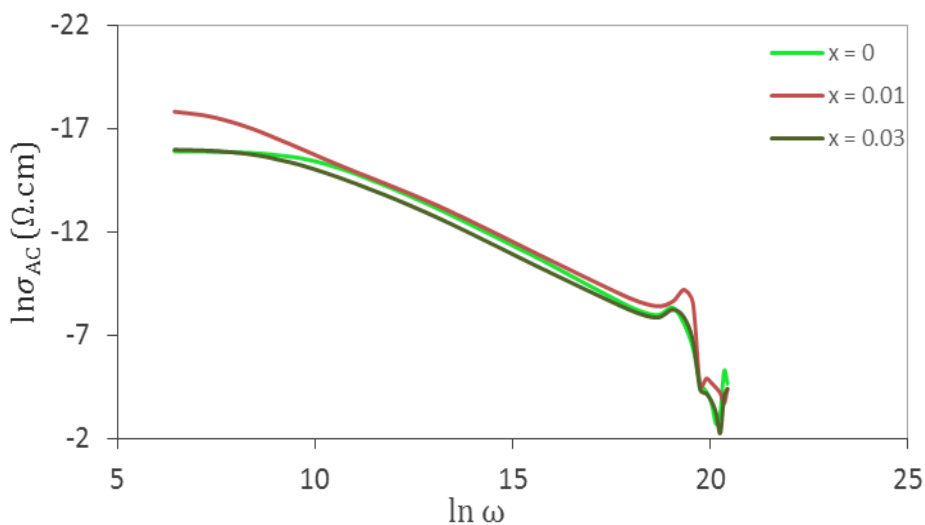


Figure 5- AC conductivity (σ_{AC}) with frequency ($ln\omega$) for $Sb_{0.4}Se_{0.6}Zn_x$ samples.

4- Conclusions

The prepared compositions retained the same orthorhombic structure but with varied lattice constants and low unit cell volume. The material possessed high absorbance in the ultraviolet region with 1% ratio of Zn^{2+} . Doping with zinc reduced the magnitudes of the energy gap. The DC electrical resistivity values showed increased semiconductor behaviour with the increase in Zn^{2+} ratio. The AC conductivity values were enhanced directly with high-frequency region (30–40 MHz) for all compound ratios used. Therefore, the results indicated potential advantages for sensor applications.

References

- [1] T. S. Kim, B. S. Chun, "Microstructure and thermoelectric properties of n- and p-type Bi_2Te_3 alloys by rapid solidification processes", *Journal of Alloys and Compounds*, vol. 43, no. 7(1-2), pp. 225-230, 2007.
- [2] X. Qiu, C. Burda, R. Fu, L. Pu, H. Chen, J. Zhu, "Hetero structured Bi_2Se_3 nanowires with periodic phase boundaries", *Journal of American Chemical Society*, vol. 126, pp. 16276-16277, 2004.
- [3] C. Mastrovito, J. W. Lekse, J. A. Aitken, "Rapid solid-state synthesis of binary group 15 chalcogenides using microwave irradiation", *Journal of American Chemical Society*, vol. 180, pp. 3262-3270, 2007.
- [4] P. Larson, R. L. Lambrecht, "Electronic structure and magnetism in Bi_2Te_3 , Bi_2Se_3 , and Sb_2Te_3 doped with transition metals (Ti–Zn)". *Physical Review B*, vol. 78, pp. 195-207, 2008.
- [5] P. Janíček, C. Drasar, P. Losták, J. Vejpravová; Transport, magnetic, optical and thermodynamic properties of $Bi_{2-x}Mn_xSe_3$ single crystals. *Physica B*, vol. 403, pp. 3553-3558, 2008.
- [6] A. Alemi, A. Klein, G. Meyer, M. Dolatyari, A. Babalou, "Synthesis of new $Ln_xBi_{2-x}Se_3$ (Ln: Sm^{3+} , Eu^{3+} , Gd^{3+} , Tb^{3+}) nanomaterials and investigation of their optical properties". *Zeitschrift für Anorganische und Allgemeine Chemie*, vol. 637, pp. 87-93, 2011.
- [7] A. Alemi, H. Hanifehpour, S. W. Joo, B. Min, "Co-reduction synthesis, spectroscopic and structural studies of novel Gd^{3+} -doped Sb_2Se_3 nanorods", *Journal of Nanomaterials*, vol. I, no. 983150, pp. 1-7, 2012.
- [8] Khawla S. Khashan, Ghosson M. Sulaimen, Sura A. Hussain, "Synthesis and characterization of Aluminum doped Zinc Oxide nano-particles by Nd:YAG laser in liquid", *Iraqi Journal of Science*, vol. 61, no. 10, 2020.
- [9] Donglou Ren, Zhuanghao Zheng, Meng Wei, "Pengcheng Zhang, Michel Cathelinaud, Hongli Ma, Xianghua Zhang; Synthesis, structure and photoelectric properties of selenide composites with in situ constructed $Sb_2Se_3/NaSbSe_2$ heterojunction", *J. of the European ceramic society*, vol. 40, no. 13, pp. 4517-4526, 2020.
- [10] K. Y. Rajpure, C. D. Lokhande, C. H. Bhosale, "Effect of the substrate temperature on the properties of spray deposited Sb–Se thin films from non-aqueous medium", *Thin Solid Films*, vol. 311, no. 1–2, pp. 114-118, 1997.
- [11] Y. Rodriguez-Lazcano, Y. Pena, M. T. S. Nair, P. K. Nair, "Polycrystalline thin films of antimony selenide via chemical bath deposition and post deposition treatments", *Thin solid Films* vol. 493, no. 1, pp. 77-82, 2005.
- [12] Y. Rodriguez-Lazcano, L. Guerrero, O. G. Daza, M. T. S. Nair, P. K. Nair, "Antimony chalcogenide thin films: chemical bath deposition and formation of new materials by post deposition thermal processing", *Superficies y Vacio*, vol. 9, pp. 100-103, 1999.
- [13] Eman A. Fadhil, Manal M. Abdullah, "CdSe / ZnS core / shell for luminescent solar concentrator", *Iraqi Journal of Science*, vol. 61, no. 7, 2020.
- [14] Oliver S. Hutter, Laurie J. Phillips, Ken Durose, Jonathan D. Major, "6.6% efficient antimony selenide solar cells using grain structure control and an organic contact layer", *J. solar energy materials and solar cells*, vol.188, pp.177-181, 2018.
- [15] Kai Zeng, Ding- Jaing Xue and Jaing Tang, "Antimony selenide thin film solar cells", *J. of semiconductor science and technology*, vol. 31, no. 6, 2016.
- [16] Xiaobo Hu, Jiahu Tao, Shiming Chen, Juanjuan Xue, Guoen Weng, Kaijiang, Zhigao Hu, Jinchun Jiang, Shaoqiang Chen, Ziqiang Zhu, Junhao Chu, "Improving the efficiency of Sb_2Se_3 thin film

solar cells by post annealing treatment in vacuum condition”, *J. of solar energy materials and solar cells*, vol.187, pp. 170-175, 2018.

- [17] Donglou Ren, Zhuanghao Zheng, Meng Wei, Pengcheng Zhang, Michel Cathelinaud, Hongli Ma, Xianghua Zhang, “Synthesis, structure and photoelectric properties of selenide composites with in situ constructed Sb₂Se₃/NaSbSe₂ heterojunction”, *J. of the European ceramic society*, vol. 40, no. 13, pp. 4517-4526, 2020.